

AUTOMATIC TOOL ALIGNMENT OF AN EYE-IN-HAND MANIPULATOR FOR OVERHEAD LINE INSULATION CLEANING

Mohit Vohra^{1,†,*}, Amrut Panda^{1,†}, Prashanth Subramaniam¹, Thani Althani¹, Mahmoud Rezk¹

¹Dubai Electricity & Water Authority, Dubai, U.A.E

ABSTRACT

The maintenance of electrical insulators is critical for ensuring the reliability and safety of power transmission networks. Traditional manual cleaning methods, while effective, pose safety risks to workers and require considerable time, compromising operational efficiency. Addressing these challenges, this paper introduces a dual-mode, eye-in-hand depth camera-based robotic system tailored for the cleaning of insulators. The system leverages a combination of automatic and teleoperated modes to optimize both safety and cleaning efficacy. In the automatic mode, the system uses advanced visual servoing techniques to detect and perform coarse alignment of the robotic end-effector with the target insulator. Following this initial alignment, control is seamlessly transitioned to the teleoperated mode, enabling precise manipulation of the cleaning tools by an operator from a safe distance. This dual-mode approach merges the reliability and speed of automated technologies with the precision and flexibility of manual control. The paper provides an in-depth analysis of the system's architecture, details the integration of its control modes, and describes the operational procedures involved. Experimental results are presented to demonstrate the effectiveness of the entire system.

Keywords: Insulator cleaning, Robotic Arms, Dual-mode operation, Teleoperation, Visual servoing, Autonomous alignment

1. INTRODUCTION

Ensuring the integrity and efficiency of power transmission systems is dependent on the critical practice of insulator cleaning, which directly influences the reliability of energy distribution networks. Over time, the accumulation of impurities on insulator surfaces reduces their effectiveness, increasing the danger of outages and stressing the importance of rigorous cleaning practices. Traditionally, manual cleaning methods have been used,

but they represent inherent safety risks to workers, prompting the search for safer and more efficient alternatives. In response to this necessity, haptically teleoperated robotic arms have arisen as a promising alternative, offering the potential to enhance both safety and cleaning efficiency. While a fully autonomous insulator cleaning manipulator presents numerous challenges [1] and risks to the power network, a teleoperated system emerges as the preferred solution due to its ability to maintain human oversight and control. This approach combines the advantages of robotic automation with human judgment, ensuring a safer and more effective cleaning process while mitigating potential risks to the power transmission network.

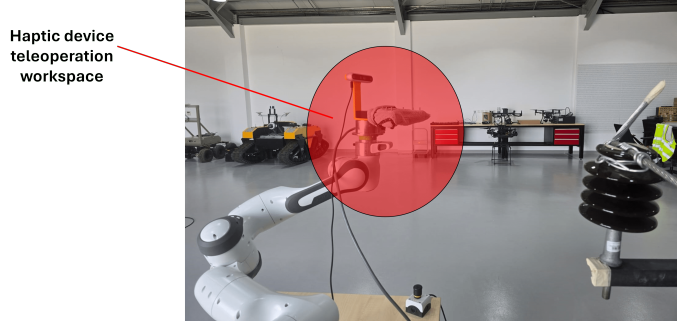


FIGURE 1: The limited workspace of haptic devices often necessitates operators to recenter frequently.

However, despite the progress made in teleoperated robotic technologies, some obstacles remain [2]. Fig. 1 shows considerable discrepancies in workspace coverage between the haptic device and the robotic arm when using haptic devices for robotic teleoperation. Haptic devices often have a much smaller workspace than the robotic arm, causing operators to quickly face the device's limits. While suitable mapping allows for comprehensive coverage of the robotic workspace, significant differences in velocity, position, and force feedback between the haptic device

[†]Joint first authors

*Corresponding author

Documentation for asmeconf .cls: Version 1.37, February 25, 2025.

and the robotic arm complicate teleoperation. Consequently, operators frequently need to reposition the haptic device's location when they reach its limits [3]. In activities such as insulator cleaning, where exact alignment is critical, operators require additional training and spend a significant amount of time correctly aligning the end-effector. Though base movement can help relieve this difficulty, terrain impediments and vehicle movement constraints continue to impede movements, relying significantly on the operator's experience. Furthermore, putting the end-effector close to the insulator presents safety problems, which originate from the robot's moving to obtain the appropriate configuration or probable controller failure. To overcome these obstacles and increase efficiency, automatic tool alignment becomes critical.

Hence to tackle the above challenges, we present a dual-mode eye-in-hand robotic system capable of switching its execution operation from automatic mode to teleoperated mode for the task of insulator cleaning. Further, the system is integrated with a visual servoing module to automatically position its end-effector in such a position, so that the insulator falls within the teleoperated range of the end-effector. At this state, the control switches from automatic to teleoperated mode for precise cleaning task. Hence, the major contributions of this paper are as follows:

- A dual-mode eye-in-hand robotic system capable of switching from autonomous mode to teleoperated mode.
- The system is integrated with visual servoing module for automatic alignment with the target insulator.
- The extensive experiments to evaluate the robotic system's performance.

The remainder of this paper is organized as follows. Sec. 2 provides the overview of the related work in the context of this paper. Sec. 3 provides a detailed overview of our system and its overall workflow. Sec. 4 provides experimental evaluation and finally, Sec. 5 concludes the paper.

2. RELATED WORK

Related work in the field includes a variety of novel techniques to improving efficiency and safety across several domains. Robotic insulator cleaning offers a viable method for preserving the integrity of power distribution networks, assuring maximum performance while reducing the dangers associated with physical intervention. Meanwhile, the use of Teleoperated Manipulator Applications provides intricate control and manipulation in hazardous areas, posing both opportunities and obstacles in its application. Furthermore, the use of Visual Servoing techniques improves robotic capabilities by providing exact visual feedback for activities that need dexterity and accuracy. These developments contribute to the progress of robotics by solving complicated real-world problems with technological ingenuity.

2.1 Robotic cleaning of insulators

Robotic insulator cleaning is essential for maintaining industrial facilities. Automated systems have modernized the process, making it more efficient and precise. Several systems have been developed to identify and recognize the insulators among the overhead power lines based on aerial imagery [4]. Crawler and

manipulator robots are predominantly used for the inspection and maintenance of overhead live-line systems as they traverse along the power line [5, 6]. Researchers have used manipulators retrofitted onto lifts for direct interaction with live power lines, typically employing two or more manipulators [7]. Water-based cleaning techniques in the drone-robot system for insulator chain maintenance on power lines signify a noteworthy advancement in automated maintenance for transmission systems. This approach boosts operational efficiency and safety through the use of advanced technologies such as depth cameras and electronic control systems [8]. A dedicated cleaning robot system is proposed for suspension insulator strings, employing a dry cleaning method to enhance efficiency and safety in insulator maintenance [9]. Experimental validation confirms the system's autonomous operation and effective cleaning performance, emphasizing its important role in preventing power failures. The robotic system [10] features a multi-arm configuration situated on an aerial platform, facilitating precise manipulation of manipulators for the cleaning of vertical insulators, utilizing dual sets of high-pressure nozzles to ensure effective cleaning procedures in the context of insulator maintenance.

2.2 Visual Servoing

There are different types of servoing methods that are mentioned in the literature such as tactile serving [11], which depends on the physical touch feedback from the machine, and visual serving [12] which is a method of controlling a robot from features extracted from real-time image streaming.

Visual servoing is mainly categorized between position-based visual servoing (PBVS) and image based visual servoing (IMVS) [13]. PBVS is a robot positioning technique dependent on the minimization of the difference between the target and current poses estimated from captured images. On the other hand, IBVS is dependent on the difference of features extracted from current and target images. With the advancement in computer vision and the re-introduction of Convolutional neural networks, there have been several advancements in the field of servoing [14–16]. Bateux et al [14], for instance, positioned an eye-in-hand manipulator in different light conditions and occlusion by depending on the features extracted from Alexnet [17] and VGG16 [18] deep learning networks. Other introduced their own deep learning architectures that assisted in increasing the positioning accuracy such as the work done by Yu et al [19] and Fuyuki et al[20].

3. METHOD

In this section, we present the workflow and provide the technical details of each modules of our dual-mode robotic system for the task of insulator cleaning.

3.1 Workflow

In this section, we outline the dual-mode operational workflow of our robotic system specifically designed for the task of insulator cleaning. This dual mode capability allows the robotic system to toggle between automatic and teleoperated control, optimizing efficiency and precision throughout the cleaning process. The workflow, depicted in Fig. 2, incorporates four main steps.

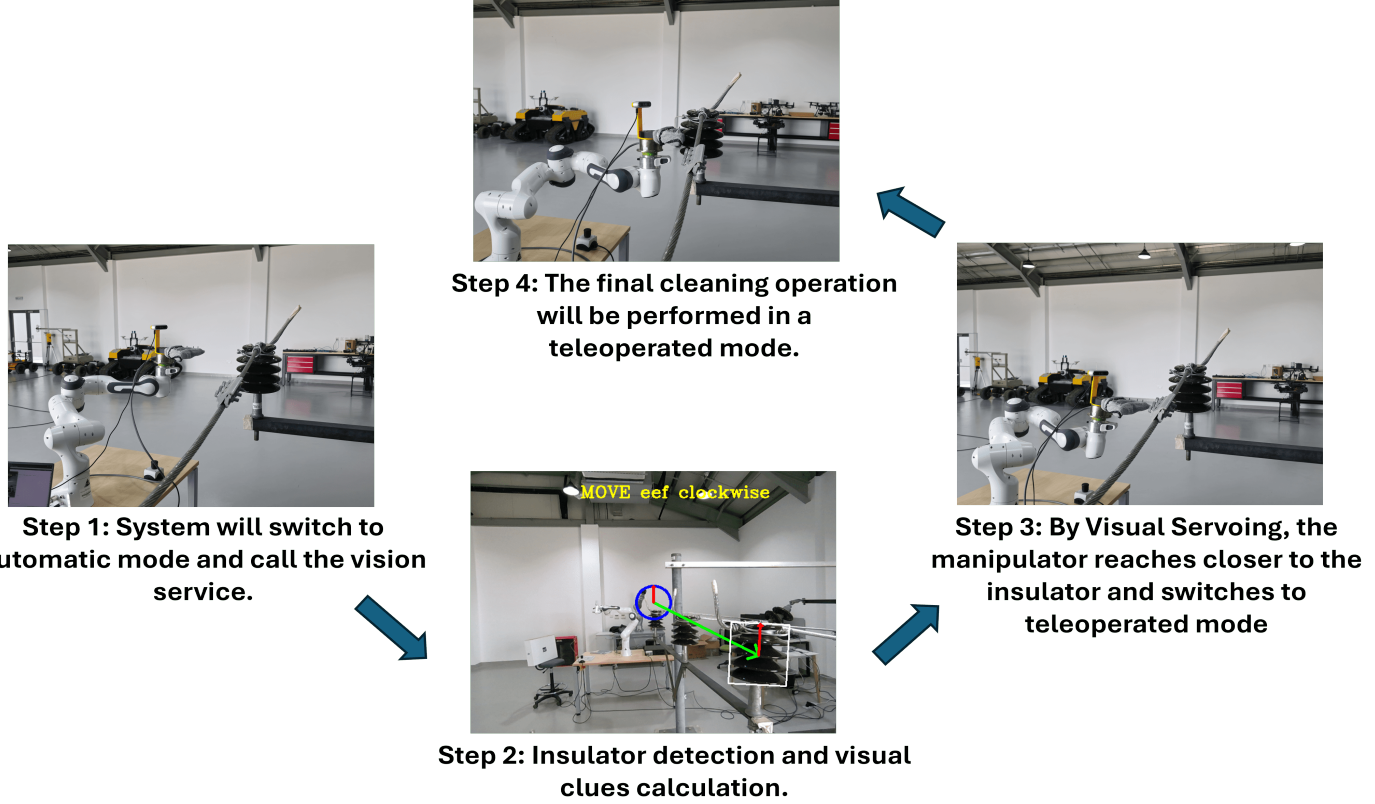


FIGURE 2: The Workflow of the system.

Step 1: Initial Positioning — At this initial stage, the robotic system is positioned so that the insulators are within the field of view of its RGB camera. At this state, the target insulator is not within the range of the haptically teleoperated end-effector’s workspace.

Step 2: Vision Service Activation — Once the robotic system is positioned at the initial pose, it engages a vision service to detect the insulators and calculate visual clues essential for precise movement. These clues include parameters like the position and orientation of the insulators. The specifics of these visual clues and their calculation will be further explored in section 3.2.

Step 3: Motion Coordination — Utilizing the visual clues mapped from the camera frame to the end-effector frame, the robot adjusts its position and orientation accordingly. This step involves a dynamic feedback loop where the robot alternates between receiving visual clues (Step 2) and adjusting its position (Step 3) until the visual information indicates that the end-effector is correctly aligned. This continuous adjustment ensures high precision without manual input, right up to the point where cleaning can commence.

Step 4: Switch to Teleoperation — For the actual cleaning task, the system switches from automatic to teleoperated mode. This switch allows the operator to manually control the end-effector, enabling precise maneuvers necessary for effective cleaning. Once the cleaning is complete, the robot returns to a predefined position and reverts to automatic mode to begin the next cleaning cycle.

This dual-mode approach leverages the strengths of both au-

tomated and manual controls, ensuring that the robotic system can operate efficiently and adaptively in complex environments. The integration of these modes is pivotal for enhancing the operational reliability and effectiveness of the robotic cleaning tasks.

3.2 Object Detection and Visual Clues Calculation

Robust detection of electrical insulators in RGB images with varying backgrounds necessitates the use of deep neural network-based methods. In our pipeline, we employ YOLOv8 as the object detector, which is capable of segmenting multiple instances of the target object—namely, the electrical insulator—within the RGB image. The visual representation of the object detection and the final visual clues are illustrated in Fig. 3.

Figure 3a displays the raw RGB image fed into the YOLOv8 network. The output from YOLOv8 provides segmentation masks for all detected insulators in the image. Employing traditional computer vision algorithms, including contour extraction and plotting, we present the final processed output in Fig. 3b. Among all extracted contours, we select the one with the maximum area, which is presumed to be the most relevant insulator for subsequent operations.

The selected contour, or insulator, is further refined by approximating it with a rotated rectangle. This rotated rectangle provides crucial information about the positioning and orientation of the insulator in the image plane, essential for precise robotic manipulation. The selected insulator and its rotated rectangle are highlighted in Fig. 3c.

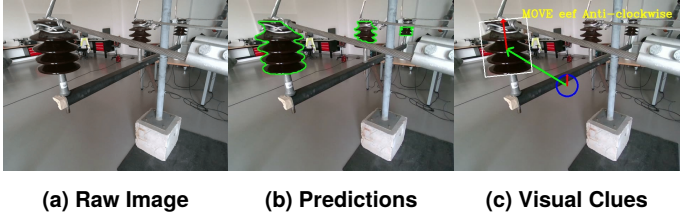


FIGURE 3: Insulator detection and Visual clues calculation.

Having selected the target insulator, we then determine two crucial visual cues: the insulator’s distance from a reference point and its alignment relative to a reference angle axis. In our setup, we define the reference point as the central point of the image, denoted by the center of the blue circle, and the reference angle axis as a vertically straight line, marked in red in Fig. 3c.

The decision to choose the image center as a reference point and a vertically straight line as a reference angle axis stems from the specific setup illustrated in Fig. 1, where the camera is mounted over the end-effector. In this configuration, aligning the insulator with the reference angle axis implies alignment with the end-effector, simplifying the cleaning task by minimizing the need for angular adjustments.

Conversely, if the target insulator significantly deviates from the reference point, understanding the direction vector from the reference point to the insulator—highlighted in green in Fig. 3c—becomes crucial. This vector guides the robotic arm’s movement, directing it toward minimizing the distance between the reference point and the insulator. Following this vector’s direction ensures the robotic arm efficiently approaches the target insulator.

By adopting this approach, the robotic system can swiftly and precisely position itself for interaction with the insulator, minimizing operational complexities and enhancing overall performance.

3.3 Visual Servoing

Visual servoing is a technique used to control the motion of a robotic system through visual feedback from a camera. In our method, depicted in Fig. 3c, we extracted two essential visual cues related to the target object: the displacement vector and its orientation with respect to a reference point and axis. To guide the robot’s movements, these visual cues need to be transformed from the camera frame to the robot’s frame. Since our application primarily focuses on teleoperated control for precise tasks, a precise transformation matrix between the camera and robot frames is not necessary. Instead, a rough approximation can be determined by measuring the distance between the camera link and the end-effector link and aligning the axes of each frame, as shown in Fig. 4. The visual cues captured in the camera frame can then be transformed into the end-effector frame using this estimated transformation. As the end-effector and control frame having a fixed and known transformation, all visual cues are then transformed into the control frame link. This enables generation of motion commands to manipulate the control frame, representing the tip of the insulator cleaning tool.

3.4 Robot Motion

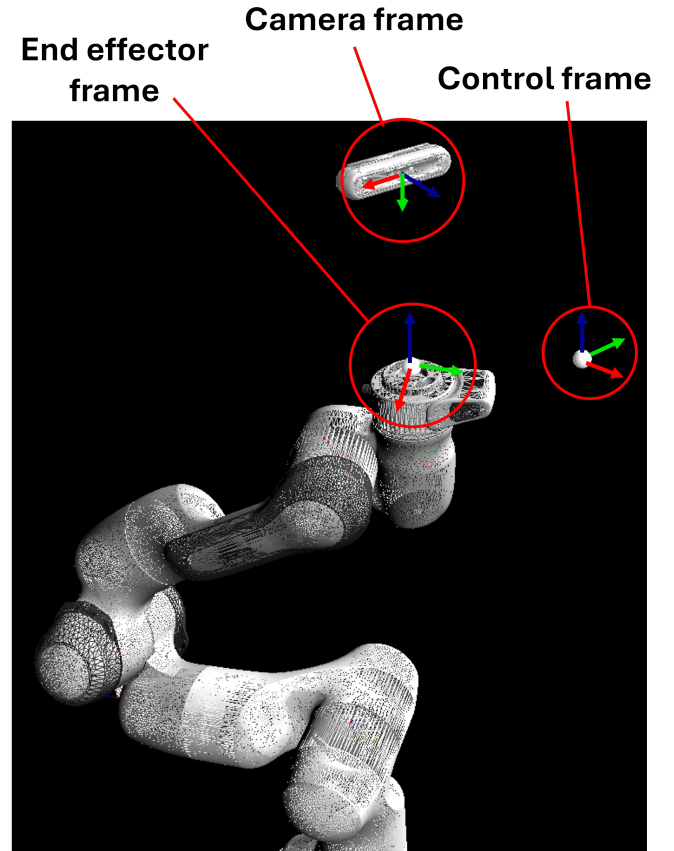


FIGURE 4: Camera frame, End-effector frame, and Control frame shown in SAI 2.0 visualizer in wireframe view

The robot motion has two modes of operation, first is the Automatic servoing mode and second is Teleoperated mode. The motion strategy of the Automatic servoing mode is as follows. We extract the rotational component of the approximate transformation matrix from the camera frame to the end-effector frame, represented by equation 1. The extracted rotation matrix is multiplied with the displacement vector to map this vector from the camera frame to the end-effector frame in order to guide the motion of end-effector. As the camera is roughly calibrated in our experiment, the constant step size is multiplied with the normalized form of mapped displacement vector represented by equation 2, and final target co-ordinates of the end-effector are calculated by equation 3.

$${}_{\text{Camera}}^{\text{EE}}\mathbf{R} = \begin{bmatrix} 0.707 & 0 & 0.707 \\ -0.707 & 0 & 0.707 \\ 0 & -1 & 0 \end{bmatrix} \quad (1)$$

$$d_{\text{EE}} = \Delta d {}_{\text{Camera}}^{\text{EE}}\mathbf{R} d_{\text{camera}} \quad (2)$$

$$x_{\text{target}} = x_{\text{current}} + d_{\text{EE}} \quad (3)$$

In the above equations, ${}_{\text{Camera}}^{\text{EE}}\mathbf{R}$ represents a rotational matrix from camera frame to end-effector frame, d_{camera} is the normalized displacement vector in the camera frame, and Δd is

the step size. d_{EE} is the displacement vector in the end-effector frame. x_{target} , the final position of the end-effector is simply the sum of the current position, $x_{current}$ and d_{EE} .

In order to execute the robotic motion, operational space framework based cartesian controllers are employed. The motion of the robotic arm causes changes in the displacement vector in turn causing motion of the end-effector. As soon as the displacement vector converges to the reference point in the camera frame, the end-effector executes a rotational motion to match the target object axis to the reference axis. Subsequently, the robot switches itself to Teleoperation mode. In any case, if the object goes out of the camera image, the robot automatically switches to teleoperation mode.

4. EXPERIMENTS

In this section, we introduce the experimental setup and delve into our observations and results obtained from the auto tool alignment experiment

4.1 Experimental Setup

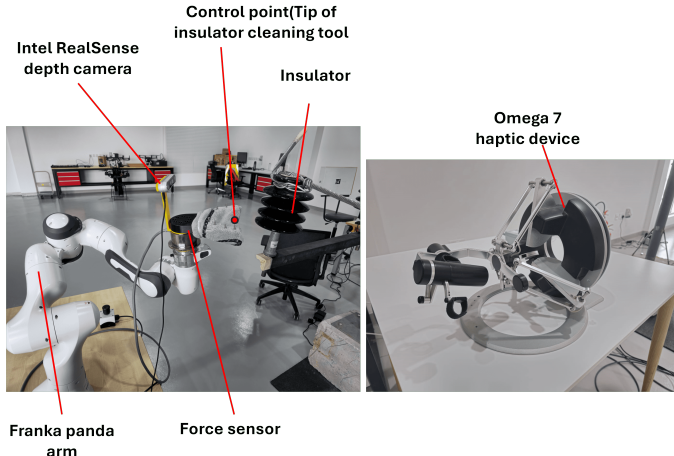


FIGURE 5: Experimental setup

We constructed a miniature setup of overhead lines, with insulators, poles and wires, to replicate a real-world configuration for our experiments. The robotic equipment used included an Intel RealSense depth camera, which captures RGBD data, and an insulator cleaning tool attached to a Franka Panda manipulator as depicted in Figure 5. The manipulator is teleoperated via the Omega 7 haptic device, which has a workspace of 160×110 mm and has a rotation range of $240 \times 140 \times 180$ degrees. It has a translation resolution of 0.01mm and rotational resolution of 0.09 degrees. This device can exert a force up to 12.0 N. Our experiments are powered by the SAI 2.0 software framework from Stanford University. The SAI 2.0 library contains control primitives for both haptic device as well as the robotic arm to facilitate the open-loop teleoperation.

For object detection and segmentation, our vision module incorporates Yolov8 by ultralytics [21], running on a NVIDIA GeForce RTX 3050 Laptop GPU with 4GB of RAM. This setup

processes images at a resolution of 640×480 pixels, with inference times around 42 milliseconds. Additional visual processing tasks, such as contour extraction and visual clues calculation, require roughly 45 milliseconds. Consequently, the vision module updates at a rate of 11 samples per second.

Communication among all system components is facilitated by a high-performance Redis server, which allows nodes to exchange data efficiently. Each node writes data to the server's database under a unique key, which can be accessed by any other node using this key. This configuration enables the robot controller node to operate at a frequency greater than 1 kHz.

4.2 Experiments and Results

To evaluate the effectiveness of our robotic system, we conducted tests across two operational modes designed for insulator cleaning: Dual Mode (combining Automatic Servoing and Teleoperated modes) and Teleoperated Mode Only. We assessed performance based on three parameters:

Success: This measures whether the end-effector successfully reached the insulator. This is crucial as the arm occasionally reaches singularity configurations that halt operations, and currently, there are no mechanisms to avoid these during motion.

Lead time: We timed how long it took for the cleaning tool mounted on robotic arm to touch the insulator from its starting position irrespective of the mode of operations, indicating the system's response speed. The robot first moves towards the insulator, realigns itself (Teleoperated or Dual mode) and finally touches the insulator for cleaning. At this instant the controller switches to cleaning mode. We register this time instant and subtract it from the initial timestamp to estimate time duration required for robot to be ready for cleaning.

Operator Convenience: This evaluates the ease of use for the operator, considering control simplicity, effort required, and overall experience. While challenging to quantify, we measured this by counting how many times the operator had to **recenter the haptic device** during the task which is defined below.

The workspace of the haptic device (Omega 7) is smaller than that of the robotic arm (Franka Emika). In our setup, we use a one-to-one position mapping between the haptic device and the robotic arm, meaning that a 5 cm movement of the haptic device results in a corresponding 5 cm movement of the robotic arm. Consequently, the robot's translation is limited by the smaller workspace of the haptic device. We intentionally implemented this one-to-one mapping to achieve high-resolution control.

During teleoperation of the Franka arm using the Omega 7, when the haptic device reaches its workspace limit (16 cm in this case), we temporarily hold the robot's position, return the haptic device to its starting position, and then resume teleoperation. This process, known as haptic recentering, allows us to continue moving the robotic arm. To cover a larger distance with the Franka arm, the haptic device must be recentered multiple times.

In order to evaluate our method, Our experimental setup involved conducting 20 rounds of cleaning tasks, each with two phases:

Dual Mode Operation: The robot first executed the cleaning task using both Automatic Servoing and Teleoperated modes. **Teleoperated Mode Only:** After the first phase, the robot was

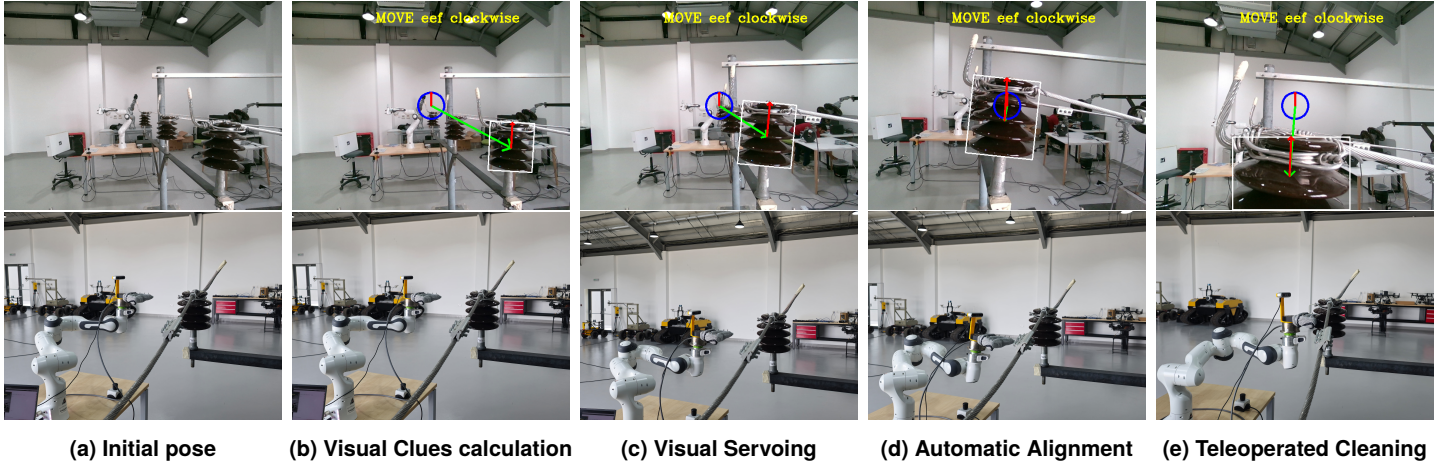


FIGURE 6: Execution steps during the task of robotic cleaning.

Operations	Success	Lead time	No. of Haptic Recentering
Dual Mode	16	7 sec	0
Teleoperated	19	18 sec	1.1

TABLE 1: Summary of the experiments

reset to the same starting pose, and the task was repeated using only the Teleoperated mode.

Each phase was timed for how quickly the robot made contact with the insulator, and we recorded the number of times the haptic device needed recentering. To ensure consistency, the robot's starting pose was randomly selected for each round but adjusted to keep the target within the camera's field of view. An illustrative example of one such test round is shown in Figure 6. The result of our experiments is summarized in table 1.

As detailed in Table 1, our findings indicate that the success rate in Teleoperated Mode alone surpasses that in Dual Mode. This discrepancy arises because the visual servoing in Dual Mode relies on processing 2D image data, causing the end-effector to move primarily within a single plane. This restriction increases the likelihood of encountering singularity configurations [22] compared to the Teleoperated Mode, where the arm can move more freely in multiple planes.

However, despite its lower success rate, Dual Mode demonstrates significant advantages in other areas. Specifically, the average time required to reach the insulator is notably shorter in Dual Mode than in Teleoperated Mode. Moreover, the need for haptic re-centering is almost eliminated in Dual Mode, with an average of nearly zero instances compared to 1.1 in Teleoperated Mode. These aspects make Dual Mode not only faster but also more comfortable and less demanding for the operator, enhancing overall efficiency and user experience during the cleaning task.

5. CONCLUSION

This paper introduces a dual-mode operational robotic system designed for insulator cleaning tasks. The system operates in two modes: automatic servoing and teleoperation. In the

automatic servoing mode, the system utilizes visual servoing techniques to align the cleaning tool accurately. This involves extracting visual cues from images and mapping them from the camera frame to the end-effector frame. In the teleoperated mode, operators take control for precise cleaning tasks on insulators. To demonstrate the effectiveness of our proposed dual-mode robotic system, we conducted a comparative analysis with the teleoperated mode alone. Our results show that the dual mode significantly outperforms the teleoperated mode in terms of both time efficiency and operator convenience.

REFERENCES

- [1] Rosell, Jan, Suárez, Raúl and Pérez, Alexander. "Safe tele-operation of a dual hand-arm robotic system." *ROBOT2013: First Iberian Robotics Conference: Advances in Robotics*, Vol. 2: pp. 615–630. 2014. Springer.
- [2] Bong, Jae Hwan, Choi, Sunwoong, Hong, Jin and Park, Shinsuk. "Force feedback haptic interface for bilateral tele-operation of robot manipulation." *Microsystem Technologies* Vol. 28 No. 10 (2022): pp. 2381–2392.
- [3] Conti, Francois and Khatib, Oussama. "Spanning large workspaces using small haptic devices." *First Joint Eurohaptics Conference and Symposium on Haptic Interfaces for Virtual Environment and Teleoperator Systems. World Haptics Conference*: pp. 183–188. 2005. IEEE.
- [4] Wu, Qinggang and An, Jubai. "An active contour model based on texture distribution for extracting inhomogeneous insulators from aerial images." *IEEE Transactions on Geoscience and Remote Sensing* Vol. 52 No. 6 (2013): pp. 3613–3626.
- [5] Alhassan, Ahmad Bala, Zhang, Xiaodong, Shen, Haiming and Xu, Haibo. "Power transmission line inspection robots: A review, trends and challenges for future research." *International Journal of Electrical Power & Energy Systems* Vol. 118 (2020): p. 105862.
- [6] Cho, Byung-hak, Byun, Seung-hyun, Park, Joon-young and Kim, Jin-Seok. "Development of automatic inspection robot for live-line insulators." *ESMO 2006-2006 IEEE*

- 11th International Conference on Transmission & Distribution Construction, Operation and Live-Line Maintenance.* 2006. IEEE.
- [7] Du, Liang and Zhang, Weijun. "A teleoperated robotic hot stick platform for the overhead live powerline maintenance tasks." *2019 IEEE 4th International Conference on Advanced Robotics and Mechatronics (ICARM)*: pp. 643–648. 2019. IEEE.
- [8] Gonçalves, Rogério Sales, De Oliveira, Murilo, Rocioli, Murilo, Souza, Frederico, Gallo, Carlos, Sudbrack, Daniel, Trautmann, Paulo, Clasen, Bruno and Homma, Rafael. "Drone–Robot to Clean Power Line Insulators." *Sensors* Vol. 23 No. 12 (2023): p. 5529.
- [9] Park, Joon-Young, Cho, Byung-Hak, Byun, Seung-Hyun and Lee, Jae-Kyung. "Development of cleaning robot system for live-line suspension insulator strings." *International Journal of Control, Automation and Systems* Vol. 7 No. 2 (2009): pp. 211–220.
- [10] Yan, Yu, Jiang, Wei, Zhang, An, Li, Qiao Min, Li, Hong Jun, Chen, Wei and Lei, YunFei. "Research on configuration design and operation effect evaluation for ultra high voltage (UHV) vertical insulator cleaning robot." *Industrial Robot: the international journal of robotics research and application* Vol. 47 No. 1 (2020): pp. 90–101.
- [11] Sutanto, Giovanni, Ratliff, Nathan, Sundaralingam, Balakumar, Chebotar, Yevgen, Su, Zhe, Handa, Ankur and Fox, Dieter. "Learning latent space dynamics for tactile servoing." *2019 International Conference on Robotics and Automation (ICRA)*: pp. 3622–3628. 2019. IEEE.
- [12] Dewi, Tresna, Risma, Pola, Oktarina, Yurni and Muslimin, Selamat. "Visual servoing design and control for agriculture robot; a review." *2018 International Conference on Electrical Engineering and Computer Science (ICECOS)*: pp. 57–62. 2018. IEEE.
- [13] Hutchinson, S., Hager, G.D. and Corke, P.I. "A tutorial on visual servo control." *IEEE Transactions on Robotics and Automation* Vol. 12 No. 5 (1996): pp. 651–670. DOI [10.1109/70.538972](https://doi.org/10.1109/70.538972).
- [14] Saxena, Aseem, Pandya, Harit, Kumar, Gourav, Gaud, Ayush and Krishna, K. Madhava. "Exploring Convolutional Networks for End-to-End Visual Servoing." (2017). URL [1706.03220](https://doi.org/10.1109/ICRA.2017.8050502).
- [15] Bateux, Quentin, Marchand, Eric, Leitner, Jürgen, Chaumette, François and Corke, Peter. "Training Deep Neural Networks for Visual Servoing." *2018 IEEE International Conference on Robotics and Automation (ICRA)*: pp. 3307–3314. 2018. DOI [10.1109/ICRA.2018.8461068](https://doi.org/10.1109/ICRA.2018.8461068).
- [16] Yu, Cunjun, Cai, Zhongang, Pham, Hung and Pham, Quang-Cuong. "Siamese Convolutional Neural Network for Sub-millimeter-accurate Camera Pose Estimation and Visual Servoing." (2019). URL [1903.04713](https://doi.org/10.1109/ICRA.2019.8856213).
- [17] Krizhevsky, Alex, Sutskever, Ilya and Hinton, Geoffrey E. "Imagenet classification with deep convolutional neural networks." *Advances in neural information processing systems* Vol. 25 (2012).
- [18] Simonyan, Karen and Zisserman, Andrew. "Very Deep Convolutional Networks for Large-Scale Image Recognition." (2015). URL [1409.1556](https://doi.org/10.1109/ICRA.2015.7139050).
- [19] Kingkan, Cherdskak, Ito, Shogo, Arai, Shogo, Namamoto, Takashi and Hashimoto, Koichi. "Model-based virtual visual servoing with point cloud data." *2016 IEEE/RSJ International Conference on Intelligent Robots and Systems (IROS)*: pp. 5549–5555. 2016. DOI [10.1109/IROS.2016.7759816](https://doi.org/10.1109/IROS.2016.7759816).
- [20] Tokuda, Fuyuki, Arai, Shogo and Kosuge, Kazuhiro. "Convolutional Neural Network-Based Visual Servoing for Eye-to-Hand Manipulator." *IEEE Access* Vol. 9 (2021): pp. 91820–91835. DOI [10.1109/ACCESS.2021.3091737](https://doi.org/10.1109/ACCESS.2021.3091737).
- [21] Jocher, Glenn, Chaurasia, Ayush and Qiu, Jing. "Ultralytics YOLOv8." (2023). URL <https://github.com/ultralytics/ultralytics>.
- [22] Kennel-Maushart, Florian, Poranne, Roi and Coros, Stelian. "Manipulability optimization for multi-arm teleoperation." *2021 IEEE International Conference on Robotics and Automation (ICRA)*: pp. 3956–3962. 2021. IEEE.